



Galileo at Io: Results from High-Resolution Imaging

A. S. McEwen, *et al.*

Science **288**, 1193 (2000);

DOI: 10.1126/science.288.5469.1193

The following resources related to this article are available online at www.sciencemag.org (this information is current as of January 27, 2009):

Updated information and services, including high-resolution figures, can be found in the online version of this article at:

<http://www.sciencemag.org/cgi/content/full/288/5469/1193>

This article **cites 22 articles**, 7 of which can be accessed for free:

<http://www.sciencemag.org/cgi/content/full/288/5469/1193#otherarticles>

This article has been **cited by** 65 article(s) on the ISI Web of Science.

This article has been **cited by** 6 articles hosted by HighWire Press; see:

<http://www.sciencemag.org/cgi/content/full/288/5469/1193#otherarticles>

This article appears in the following **subject collections**:

Planetary Science

http://www.sciencemag.org/cgi/collection/planet_sci

Information about obtaining **reprints** of this article or about obtaining **permission to reproduce this article** in whole or in part can be found at:

<http://www.sciencemag.org/about/permissions.dtl>

Galileo at Io: Results from High-Resolution Imaging

A. S. McEwen,¹ M. J. S. Belton,² H. H. Breneman,³ S. A. Fagents,⁴
 P. Geissler,¹ R. Greeley,⁴ J. W. Head,⁵ G. Hoppa,¹ W. L. Jaeger,¹
 T. V. Johnson,³ L. Keszthelyi,¹ K. P. Klaasen,³ R. Lopes-Gautier,³
 K. P. Magee,³ M. P. Milazzo,¹ J. M. Moore,⁶ R. T. Pappalardo,⁵
 C. B. Phillips,¹ J. Radebaugh,¹ G. Schubert,⁷ P. Schuster,⁸
 D. P. Simonelli,⁹ R. Sullivan,⁹ P. C. Thomas,⁹ E. P. Turtle,¹
 D. A. Williams⁴

During late 1999/early 2000, the solid state imaging experiment on the Galileo spacecraft returned more than 100 high-resolution (5 to 500 meters per pixel) images of volcanically active Io. We observed an active lava lake, an active curtain of lava, active lava flows, calderas, mountains, plateaus, and plains. Several of the sulfur dioxide-rich plumes are erupting from distal flows, rather than from the source of silicate lava (caldera or fissure, often with red pyroclastic deposits). Most of the active flows in equatorial regions are being emplaced slowly beneath insulated crust, but rapidly emplaced channelized flows are also found at all latitudes. There is no evidence for high-viscosity lava, but some bright flows may consist of sulfur rather than mafic silicates. The mountains, plateaus, and calderas are strongly influenced by tectonics and gravitational collapse. Sapping channels and scarps suggest that many portions of the upper ~1 kilometer are rich in volatiles.

The Galileo spacecraft has been in orbit about Jupiter for over 4 years. A flyby of Io during Jupiter orbit insertion in December 1995 excluded remote sensing observations because of a tape-recorder anomaly (1). Additional close encounters to Io were deferred until the end of the Galileo Europa Mission (GEM) to minimize radiation damage to the spacecraft. Io flybys occurred on 11 October 1999 (I24), 26 November 1999 (I25), and 22 February 2000 (I27). Both I24 and I25 suffered from spacecraft or instrument anomalies that eliminated or degraded some observations (2), but more than 100 useful images with resolutions from ~10 to 500 m/pixel were returned (3). I27 was a fully successful encounter, but much of the data have not yet been returned or analyzed. The high-resolution images are centered on the antiojovian hemisphere centered at 180° longitude (Web fig. 1) (3). The best Voyager spacecraft images (0.5 to 2 km/pixel) were acquired on the subjovian hemisphere from 250° longitude westward to 50° longitude. Color coverage of the antiojovian

hemisphere at 1.25 km/pixel was acquired in orbit C21 (2 July 1999), providing regional context for the high-resolution images (Fig. 1).

Relatively distant monitoring of Io by Galileo in 1996–99 provided important insights into the volcanic plumes, atmosphere, surface changes, hot spots, composition, and large-scale distribution of landforms (4–9), but high-resolution images are required for detailed interpretations of surface processes. We planned observations to investigate how the volcanoes erupt and modify the landscape, the composition of the lavas, and how the enigmatic landforms are created and modified.

Some of the most important new results are nondetections. No impact craters have been identified, even at high resolution, confirming the young age (<1 million years) of Io's surface (10). There has also been no evidence for thick, viscous lava flows or steep-sided domes, suggestive of evolved, silica-rich compositions. This confirms previous evidence that Io's volcanism is dominated by mafic eruptions and that Io probably lacks the low-density, silica-rich crust that was expected to result from magmatic differentiation (11).

Pele. Several characteristics of Pele (12) make it unique among Io's volcanic centers. It has a 1200-km-diameter circular deposit with a bright red color that is deposited by a plume more than 400 km high (13). The plume is now known to be rich in S₂ gas as well as SO₂ (14). We suspect that other diffuse, red deposits on Io consist of short-chain sulfur species formed from condensation of S₂-rich volcanic gases (6). Pele is also

the source of the most stable high-temperature hot spot on Io, having almost the same high intensity at near-infrared wavelengths in every Galileo observation (5). Because the hot area is nearly constant over time and does not lead to larger cooler areas like advancing lava flows, it was surmised that Pele is an active lava lake (15). Multifilter SSI experiment data combined with spectra from the Near-Infrared Mapping Spectrometer (NIMS) suggested peak surface temperatures of ~1300 K (9, 15). However, this is only a lower limit to the actual lava temperature, which is expected to be at least 100 K higher (16).

The nighttime I24 observation of Pele was acquired to test the lava lake hypothesis and to better constrain the lava temperature. The images show a discontinuous curving line glowing in the dark (Fig. 2). The intensity of the glow translates to a brightness temperature of about 1000 K. The shape and size of this glowing line are consistent with the margin of the Pele caldera. We interpret the bright line as exposures of molten lava where a crust over the lava lake breaks up when pushed against the caldera walls. However, the thermal radiation detected in these images is only a small fraction (<1%) of that usually emitted by Pele. Low-resolution images taken less than 1 day after the high-resolution I24 observation showed Pele to be as active as usual. We suspect that localized active fountaining, which would explain the bulk of the short-wavelength thermal emission, was missed by the images.

Pillan. An eruption near Pillan Patera in June 1997 produced a 400-km-diameter deposit of dark, diffuse material (4). A 70-km-long dark lava flow formed to the north of Pillan Patera at the same time. Subsequent changes have been seen over the past 2 years (17). A joint SSI and NIMS eclipse observation of Pillan on 27 June 1997 provided a temperature estimate for the lavas of at least 1800 to 1900 K, suggesting an ultramafic composition (9, 15). Thermal observations are consistent with a lava coverage rate of ~330 m² s⁻¹, so most of the new flows were probably emplaced in about 2 weeks (15). The temperature-area distribution changed markedly between 1997 and 1999, consistent with cooling flows from the 1997 eruption, and a large (150 km high) plume seen in 1997 is no longer detectable.

In I24, we obtained a strip of high-resolution images to investigate the morphology of the 1997 lava flow (Fig. 3). The images show a complex mix of pits, domes, channels, and possibly rafted plates. Channels and rafted plates may indicate rapid emplacement of lava because a stable insulating crust did not have an opportunity to form or was disrupted by a surge in flow rate (18). These dark flows were still warm in I24 (19). The pits and domes, which range from a few tens of meters to many hundreds of meters in scale, are more difficult to explain.

¹Lunar and Planetary Laboratory, University of Arizona, Tucson, AZ 85721, USA. ²National Optical Astronomy Observatories, Tucson, AZ 85719, USA. ³Jet Propulsion Laboratory, Pasadena, CA 91109, USA. ⁴Department of Geology, Arizona State University, Tempe, AZ 85287, USA. ⁵Department of Geological Science, Brown University, Providence, RI 02913, USA. ⁶NASA Ames Research Center, Moffett Field, CA 94035, USA. ⁷Department of Earth and Space Sciences, University of California, Los Angeles, Los Angeles, CA 90095, USA. ⁸DLR, Institut für Weltraumsensorik und Planetenerkundung, 12489 Berlin, Germany. ⁹Center for Radiophysics and Space Research, Cornell University, Ithaca, NY 14853, USA.

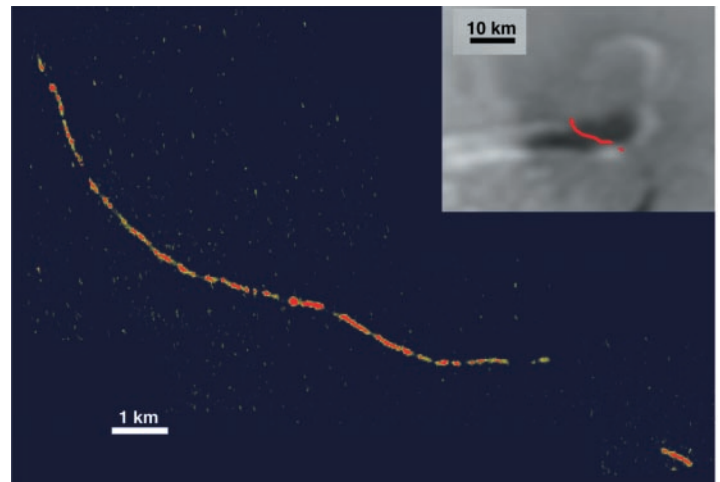
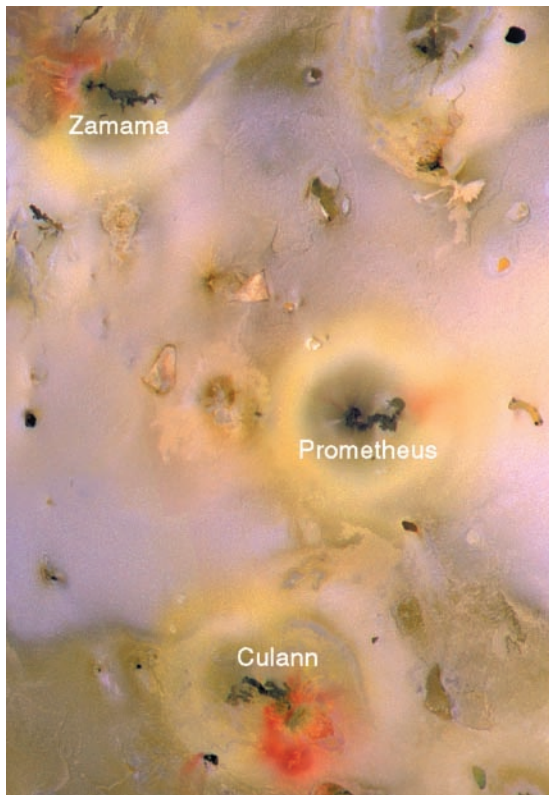


Fig. 1. (Left) Portion of a full-disk color mosaic from orbit C21, 1.25 km/pixel. Image width = 1000 km. Colors are enhanced. **Fig. 2. (Right)** Bright (hot) margin of the Pele caldera imaged in the dark, and the estimated location of the bright margin overlain in red on the best daytime image of Pele (inset). Oblique images (25° emission angle) reprojected to nadir view; 30 m/pixel scale.

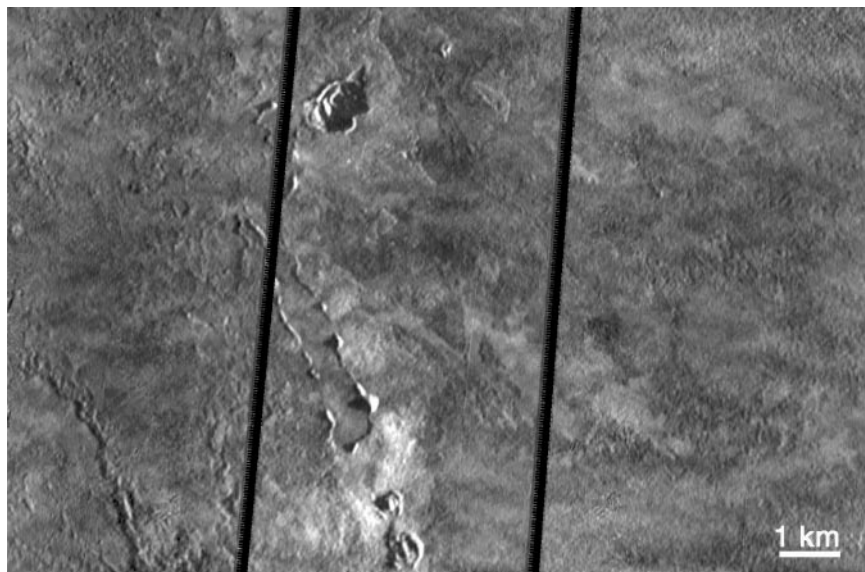


Fig. 3. Portion of high-resolution (19 m/pixel) mosaic strip over 1997 lava flows north of Pillan Patera. The shadow on the possible flow margin at bottom left indicates a thickness of ~10 m. Dark bands are areas where the scrambled images cannot be reconstructed (2).

One possibility is that these are the result of interactions between the hot lava and a volatile-rich substrate. Such vents would be analogous to terrestrial rootless cones (20), because the actual source of the lava is tens of kilometers to the north.

Most dark lava flows and calderas on Io have a shallow spectral absorption feature near 900 nm, consistent with Mg-rich silicates such as orthopyroxene (6). Full-disk color coverage

obtained in I24 showed that the dark diffuse deposits surrounding Pillan also display the 900-nm absorption, suggesting the presence of silicate pyroclastics. This is the first evidence that silicate particles may be carried to heights of over 100 km in Io's plumes.

Zamama. A new ~100-km-long dark flow field and a ~75-km-high plume named Zamama appeared between the Voyager flybys and Galileo's first images of Io (4). The plume

and the thermal emission from Zamama have varied in brightness over the past 4 years (5). An observation in March 1998 (see 3 July 1998 cover of *Science*) showed the plume erupting from the center of the dark flow field. A strip of images at 35 to 40 m/pixel (Fig. 4) and a context image (400 m/pixel) over the entire flow field were obtained in I24 to examine the relations between the plume, lava flows, and the diffuse red material extending west from Zamama (Fig. 1). The new images revealed the existence of the primary vent at the westernmost end of the dark flows. Lava flows form a radial pattern around this vent, and the red deposit emanates from this point. The main Zamama flow field extends to the east from a 25-km-long fissure on the flank of the primary vent. The high-resolution strip shows that some of the lava flows radial to the primary vent have channels with bright floors. These channels may have been carved by silicate lava (and later covered by bright material) or by remobilized sulfur-rich materials. Both ultramafic and sulfur lavas on Io are predicted to be turbulent and could carve channels (21). The main flow field has a uniformly dark surface and an intricately crenulated flow margin, characteristics of inflated pahoehoe sheet flows (22). The vent region for the Zamama plume is within the eastern flow field and does not issue from the primary vent.

Prometheus. Prometheus is a plume visible in every observation sequence by the Voyager and Galileo spacecraft. It has also been a persistent high-temperature hot spot during Galileo's tour of Jupiter (5). Although the plume has

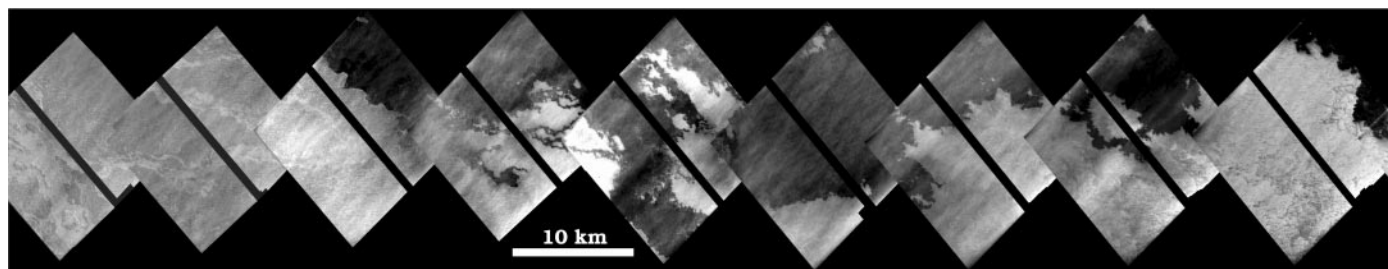


Fig. 4. Zamama: high-resolution (30 m/pixel) strip of images located along the southern margin of the dark flow field. Dark bands are areas where the scrambled data cannot be recovered, and the streaks from lower left to upper right are artifacts from the reconstruction (2).

been stable in size, shape, and optical properties, its source moved about 75 to 95 km to the west between the times of the Voyager flybys in 1979 and Galileo's first images in 1996 (4). The images also showed a new dark flow extending between the Voyager-era and Galileo-era plume source locations (Fig. 1). Two competing ideas were developed to explain these observations. First, the Galileo-era plume might be the product of a separate volcano with a bright plume that was coincidentally similar to the Voyager-era plume, and either the Galileo-era or Voyager-era vent also produced a flow field that moved into the other vent region. Second, the main source of silicate lava may be unchanged since Voyager, and the plume is generated near the front of the flow field. As a result of the lava flows advancing to the west, the plume source also moved, either continuously or episodically. Migration of the plume vent location has not been detected in the 3.5 years of Galileo observations (17), consistent with either a new silicate source or episodic movement associated with the advancing lava.

Observations in I24 and I27 were planned to address this mystery of the wandering plume. The new images show that the Prometheus flow field is built up of a patchwork of dark, kilometer-scale lobes with intricately crenulated flow margins characteristic of compound inflated pahoehoe flows (22). Changes in the shapes and locations of dark lobes between October 1999 and February 2000 (Fig. 5) are interpreted as due to advancing flow lobes. Dark areas in the I27/I24 ratio image are new dark flows, whereas bright patches are where flows that were dark in I24 have faded. Hot lava flows are dark because they are not covered by the bright SO_2 -rich plume deposits. Note the juxtaposition of the dark and bright areas in the ratio image, which indicates that most of the fresh flows seen in I27 are extensions of the flows seen active in I24. About 60 km² was covered by new lava flows in the 134 days between the two images, and a similar amount of dark lava has faded. The average areal coverage rate at Prometheus is about 10 times higher than that at Kilauea (23). New lava is primarily erupting onto other recent flows rather than expanding the flow field further into the bright plains.

The new images also revealed the presence of a caldera north of the Voyager vent region,

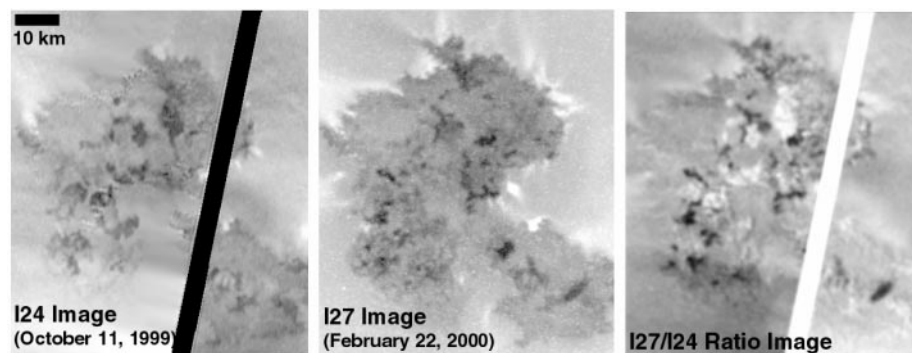


Fig. 5. Changes at the western end of the Prometheus lava flows between orbits I24 and I27. Both images were taken with the green filter and have a resolution of about 180 m/pixel. The I24 image was originally garbled (2); the dark band is where the data could not be reconstructed. Another problem that could not be corrected is manifested as patches of the image that are blurred. The ratio image is constructed by dividing the I27 image by the I24 image.

and NIMS thermal mapping revealed two main hot spots: one just south of the caldera and the other within the western flow field and corresponding to the Galileo-era plume vent region (24). Combining these data, we created a description of the eruption at Prometheus (Web fig. 2). The magma is stored in an underground chamber beneath the caldera, and the lava reaches the surface through a fissure about 15 km to the south. A streak of red material extends east from this vent. From analogy with Pele, we think that the red deposits condense from gas containing S_2 (14), and the observations at Pele, Zamama, Prometheus, and Culann suggest that S_2 emanates from the sources where silicate lava erupts onto the surface. From its source, the lava travels about 80 km west through lava tubes to multiple active flow lobes. The exposed liquid lava produces the large, high-temperature area mapped by NIMS (24) on the western end of Prometheus. A 100-km-high plume rich in sulfur dioxide-rich gas (7, 24) rises above these active lava flows. The I24 and early I27 images do not show any evidence for a specific vent for the plume, and bright streaks suggest multiple vents around the flow margins. Kieffer *et al.* (25) address the challenge of explaining how the steady eruption behavior could result from an active lava flow interacting with volatile-rich ground.

Emakong Patara. Along with >100 thermally active volcanic centers, Io has many regions of recent volcanic activity with no ob-

served high-temperature anomaly. Many of these regions have associated lava flows that are bright, as opposed to the dark flows associated with high-temperature hot spots. Emakong is one of the largest examples of a caldera with associated bright lava flows, where no hot spot has been detected. The I25 observations were planned primarily to provide stereo topographic information on the rim of the caldera and what appeared to be the scarp of a thick lava flow to the east. Unfortunately, the spacecraft safing during I25 eliminated the first half of the stereo observation. However, the remaining observation (Fig. 6) shows that the "scarp" is actually the margin of a bright, channel-fed, lava flow with no discernible relief. The margins of this bright flow are convoluted, indicating that the lava was able to move through narrow topographic constrictions or experienced numerous small breakouts, consistent with a low-viscosity liquid. A contender for the composition of this bright, low-viscosity lava is sulfur. Although Galileo has frequently detected the high-temperature silicate flows, sulfur flows may nevertheless be a major component of the surface. Fresh bright flows cover ~2% of the surface, similar to the coverage by dark flows (Fig. 1).

Tvashtar Catena. The Tvashtar observation was intended to examine the morphology of some of the largest calderas on Io. A hot spot had been previously seen in the region only once (4). However, Galileo caught the onset of a new volcanic eruption episode within the chain of

GALILEO: IO UP CLOSE

nested calderas (Fig. 7). The fresh lava was hot enough, and thus bright enough, to overload SSI's charge-coupled device detector, leading to "bleeding" of electrons and columns of saturated pixels. Because of the way electrons are transferred within the detector, most of the bleeding extends down the frame, a small amount of bleeding occurs upward, and none takes place laterally. This allowed us to partially reconstruct the distribution of hot pixels that produced the bleeding. The hot lava appears to be issuing from an E-W-oriented linear fissure that is located at the base of a scarp on the caldera floor. If we assume that the fissure is linear, then the calculated position is consistent with hot lava rising to ~ 1.5 km above the

fissure. In other words, it appears to be a lava curtain (a line of lava fountains). Tvashtar was also observed by ground-based telescopes while located near the limb (26). Other short-lived, high-temperature hot spots seen near the limb were interpreted as possible lava fountains (27). The minimum temperature of the exposed lava in the western half of the Tvashtar fissure is 1120 K as seen by NIMS (24), and ground-based observations 36 hours later indicate temperatures of at least 1300 to 1900 K (26).

New eruptive episodes of mafic volcanism on Earth commonly begin with a curtain of lava along a fissure, but the sources rapidly (in hours to days) contract into localized vents. The lower gravity and atmospheric pressure and higher lava

temperatures imply that a given volatile content will produce a fountain that is of order 100 times higher on Io than on Earth (28). The driving volatiles on Io are probably SO_2 and/or sulfur rather than H_2O or CO_2 . Sulfur solubility in silicate melts is difficult to quantify, but even low volatile contents may lead to magma fragmentation and fountaining. With the use of models for the ascent and eruption of lavas on various planets, an eruption rate per unit length of the fissure of 0.7 to $7 \text{ m}^3 \text{ s}^{-1} \text{ m}^{-1}$ was calculated (29). This assumes that 0.1- to 1-mm spheres are ejected up to 30 km by gases exiting the vent at $\sim 500 \text{ m s}^{-1}$ (30). For comparison, analysis of an eruption on the south rim of Kilauea caldera gave $\sim 7 \text{ m}^3 \text{ s}^{-1} \text{ m}^{-1}$ (31). We also considered the rise of magma in dikes from reservoirs in the crust and mantle of Io. Marginally buoyant, low-viscosity magma in Io's crust would be expected to flow upward in a turbulent fashion at speeds of 3 to 5 m s^{-1} and would lead to volume fluxes consistent with those found from the lava fountain analysis.

Culann Paterra. One of the most colorful

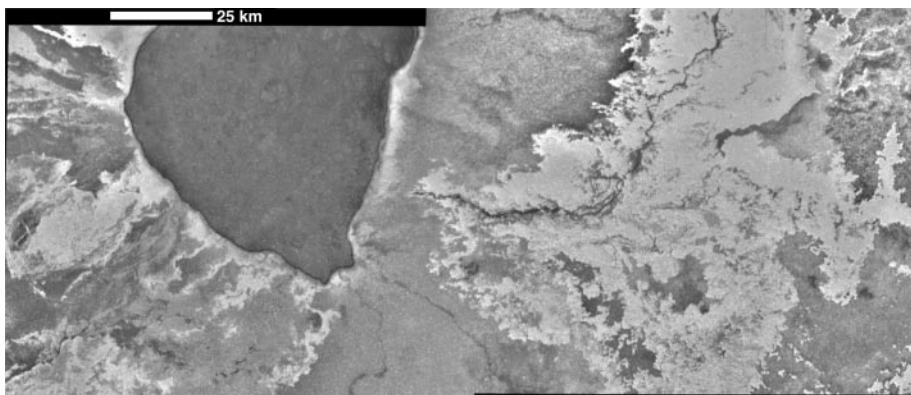


Fig. 6. Emakong Patera and lava flows at 150 m/pixel. North is 13° to the left of up.

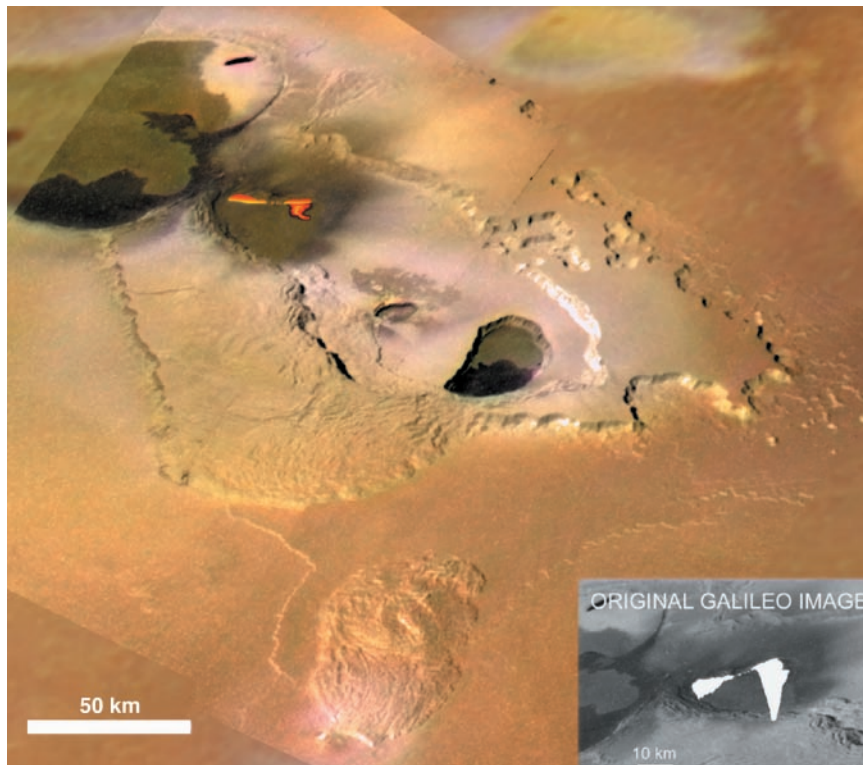


Fig. 7. Tvashtar Catena mosaic at 180 m/pixel, merged with C21 color data. The bright "bleeding" region (inset) has been replaced in the color image with an interpretive drawing showing the possible distribution of molten lava in a lava curtain along a fissure and feeding a flow to the south.

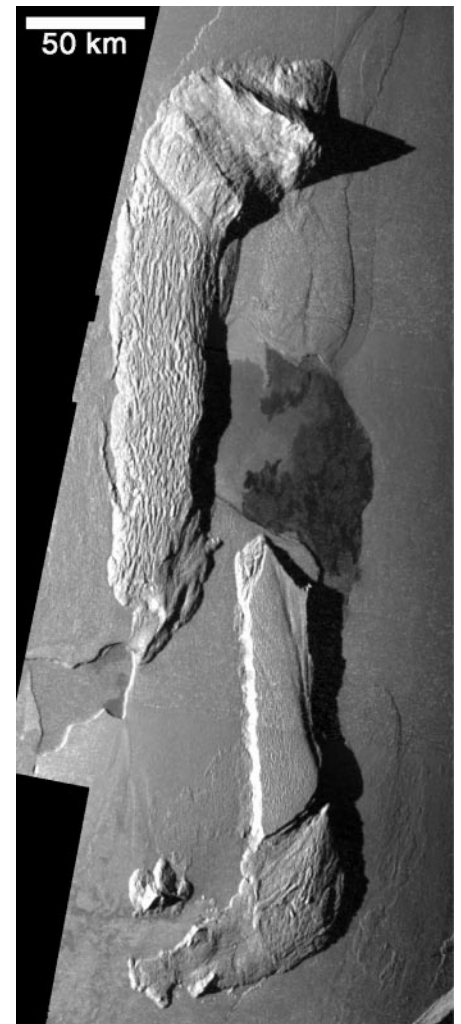


Fig. 8. Mosaic of Hi'iaka Patera and Montes at 260 m/pixel. Note the parallel structures immediately north and south of the dark lavas.

volcanic centers on Io is Culann Patera (see cover). The cover image is the best high-resolution color view of Io obtained during I24 and I25. Culann has been persistently hot during the past 4 years, and a faint plume was probably detected there in 1996 (4, 5). The color mosaic shows the complex relations between the diffuse red deposit, the more confined green deposit, and the various colored lava flows. The central caldera has a highly irregular scalloped margin and a green-colored floor. Lava flows spill out of the caldera on all sides, as at Emakong Patera (Fig. 6). A dark red, curving line extending northwest from the southwestern tip of the caldera may mark a crusted-over lava tube feeding the dark (and hot) silicate flows to the northwest (bottom left of rotated cover image). Unusual dark red flows to the southeast may be sulfur flows or silicate flows with an altered surface. Culann's caldera and several lava flows extending from the caldera are coated by greenish materials [defined as spectral units with a peak in reflectance at ~ 600 nm (6)]. The greenish units often have sharp boundaries, apparently confined to the caldera floor and the dark flows. These and other observations (17) suggest that the greenish material on Io forms as a coating on warm silicate lavas. Its distinct color may be due to contamination or alteration of the mantling material (32). The diffuse red deposit

is similar to the deposit from Pele's plume, and both plumes are nearly transparent at visible wavelengths, so we suspect similar plume compositions (SO_2 and S_2) (14, 24).

Mountains and related landforms. A number of observations were specifically targeted to investigate the enigmatic mountains on Io. Carr *et al.* (8) tabulated ~ 100 mountains and plateaus, many of which have been determined from shadow measurements or stereo photogrammetry to be several kilometers high. The highest mountain measured to date is 16 ± 2 km high (33). The mountains do not appear to be volcanoes. Instead, they often resemble tilted blocks bounded by steep scarps, a characteristic that prompted Schenk and Bulmer (33) to propose that such mountains formed by thrust faulting, which in turn is driven by a global crustal compression resulting from Io's high resurfacing rate (34). Despite the possible tectonic origin of the mountains, there is no obvious global pattern in their distribution.

The new SSI data suggest an intriguing association between mountains and calderas, which may help explain how both form. Earlier studies (with lower resolution images) reported no strong correlation between the locations of mountains and volcanic centers (8). However, 6 of 13 mountains imaged at resolutions better than 0.5 km/pixel are seen to have calderas cut

into their sides, and many of the calderas have rectilinear margins or are highly elongated (Figs. 8 and 9 and Web fig. 3). Mountains and some calderas could be genetically related. The combination of the stresses due to mantle plumes impinging on the base of the lithosphere and global compression may cause the crust to fail, allowing the formation of large mountains by thrust faulting. These fractures may then serve as conduits for magma to rise to the surface.

Some of the paterae might be better classified as tectonic depressions rather than calderas, because calderas form primarily by collapse over an evacuated magma chamber. In the case of Hi'iaka Patera (Fig. 8), it may be possible to reconstruct the relation between the tectonics and the lava-filled depression. The north and south margins of the patera can be fit together as if they were the result of the crust being laterally pulled apart. Furthermore, the two mountains bordering Hi'iaka Patera can be reconstructed into a single mountain if one assumes that the depression formed at a releasing bend in a larger transtensional fault. However, the similar shapes and heights of the patera margins and mountains could be coincidental.

The images also suggest processes by which the mountains deteriorate. Figure 9, A to C, illustrates the possible sequence of disintegration of Ionian mountains from angular peaks and scarps on the left to broad plateaus surrounded by debris aprons on the right. From shadow measurements, the mountain in Fig. 9A (adjacent to Gish Bar Patera; Web fig. 3) is 9.8 km high. Skythia Mons (Web fig. 3 and Fig. 9B), which is 4.6 km high (8), appears to be in the process of collapsing outward by landsliding.

Many Ionian mountains exhibit ridges parallel to their margins, such as the west side of Hi'iaka Mons (Fig. 8), where ridges are typically 10 km long and 2 km across and spaced ~ 4 km apart. One interpretation is that the ridges form by compression as the near-surface layer slides downslope under the influence of gravity. A sulfur-rich layer could produce a weak detachment surface. Modeling of horizontally compressed folds with ~ 1 - to 4-km wavelength suggests formation in a single competent elastic layer with a thickness of order 20 to 100 m (35). One of the highest resolution observations from I24 is of Ot Mons (Fig. 9D), showing a complex hummocky surface. The lower areas are covered with dark material. Terracing within the walls of amphitheatres appears to be layering. This image may represent how the ridges seen on mountains would appear at 9 m/pixel resolution. If so, then the ridges are breached or disrupted by poorly understood processes.

Some Ionian plateaus or mesas have smooth tops and steep, scalloped margins (e.g., Fig. 7 and cover). The scalloped margins may have

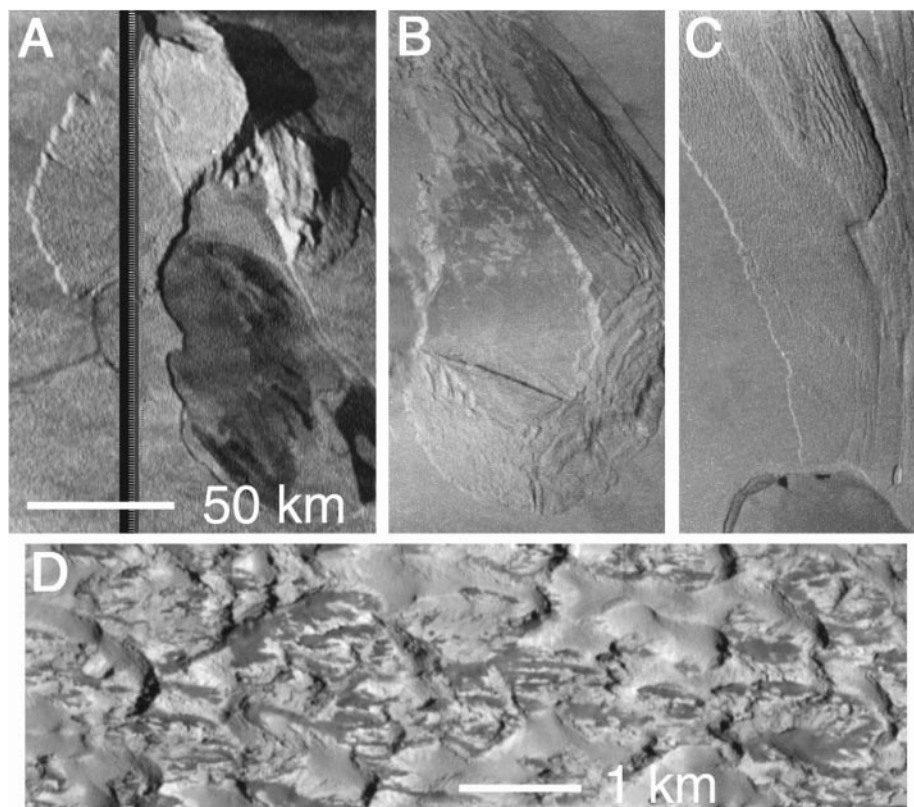


Fig. 9. (A to C) Suite of mountains (see Web fig. 3) illustrating possible age and degradation sequence from sharp, angular peaks (A) to low, ridged plateaus (C). (D) A small portion of Ot Mons imaged at 9 m/pixel. Illumination is from the west (left) in all four images; north is up in (A) to (C) and down in (D). I24 images [(A) to (C)] were reconstructed (2).

formed by gradual sapping as liquefied SO₂ seeps out at the base (36), perhaps exploiting and enlarging preexisting joints and fractures. The height of the mesa forming the eastern margin of Tvashtar Catena (Fig. 7) is ~1 km, the depth at which SO₂ is expected to become liquid (30). Diffuse white patches often appear to emanate from the bases of scarps on Io, consistent with plumes of SO₂ expected to form when the liquid reaches the triple point near Io's surface.

Discussion. The dominant eruption styles on Io may vary with latitude. At low latitudes, we see many long-lived eruptions with insulated flow fields and often associated with Prometheus-type plumes, as well as short-lived eruptive episodes (Pillan) and lava lakes (Pele). At high latitudes, the eruptions are mostly short-lived but high-volume outpourings of lava, probably with lava fountains such as that at Tvashtar (27). We have never seen an active plume at high latitudes, but we do see new color patterns indicative of short-lived plumes. One interpretation is that the lithosphere is thicker at high latitudes, such that only large batches of magma are able to ascend to the surface.

A subject of great interest for understanding global change is whether terrestrial flood lavas have been emplaced rapidly in open channels or sheet flows or relatively slowly through insulated (crusted-over) tubes or sheet flows (37). Most terrestrial flood lavas are highly eroded, so the emplacement style is contentious. On Io, we see examples of both rapidly emplaced flows (Pillan and Tvashtar) and flows emplaced over many years or decades (Zamama, Prometheus, Amirani, and Culann). These active flow fields provide important clues to the emplacement of ancient flood lavas on Earth and other planets. The formation and destruction of landforms such as mountains and calderas are also much more rapid on Io than on other planets, so Io is a unique laboratory to study processes normally inferred from the incomplete geologic record.

References and Notes

1. W. J. O'Neil et al., in *The Flight of Project Galileo as Reported Annually to the IAF/AIAA, IAF-96-Q-2.01, 1* (International Astronautical Federation, Paris, 1997).
2. The majority of the I24 images were acquired in a special mode (2 × 2 pixel summation and a fast 2.6-s readout time) designed to minimize radiation noise. We expected the radiation noise to be severe in images acquired close to Io, but the image quality proved much better than expected. Unfortunately, the summation mode, which worked correctly through orbit C21, produced garbled images in I24. Many of the images were reconstructed with an innovative algorithm devised at the Jet Propulsion Laboratory (JPL) with the LabVIEW software from National Instruments (Austin, TX). However, the photometry remains severely compromised, eliminating useful color data, and parts of some images are completely unrecoverable. Full-resolution imaging modes (no pixel summing) worked correctly, but only a few partial (top one-third) frames were acquired in I24 while close to Io. I25 and subsequent encounters were replanned to acquire only full-resolution images.
3. See www.sciencemag.org/feature/data/1049308.shl

for a table of I24 and I25 image characteristics and the Web figures.

4. A. S. McEwen et al., *Icarus* **135**, 181 (1998).
5. R. Lopes-Gautier et al., *Icarus* **140**, 243 (1999).
6. P. E. Geissler et al., *Icarus* **140**, 265 (1999).
7. P. E. Geissler et al., *Science* **285**, 870 (1999).
8. M. H. Carr et al., *Icarus* **135**, 146 (1998).
9. A. S. McEwen et al., *Science* **281**, 87 (1998).
10. T. V. Johnson and L. A. Soderblom, in *Satellites of Jupiter*, D. Morrison, Ed. (Univ. of Arizona Press, Tucson, AZ, 1982), pp. 634–646.
11. L. Keszthelyi and A. S. McEwen, *Icarus* **130**, 437 (1997); A. S. McEwen, R. Lopes-Gautier, L. Keszthelyi, S. W. Kieffer, in *Environmental Effects on Volcanic Eruptions: From Deep Oceans to Deep Space*, J. R. Zimbelman and T. K. P. Gregg, Eds. (Plenum, New York, in press).
12. Plumes have given names only (such as "Pele"), whereas surface features are called a patera (irregular or complex depression), fluctus (flow), mons (mountain), mensa (mesa), planum (plateau), or catena (chain). Most volcanic centers include several features, so in practice we often drop the feature name and refer to the entire complex by its given name.
13. J. R. Spencer et al., *Geophys. Res. Lett.* **24**, 2471 (1997).
14. J. R. Spencer, K. L. Jessup, M. A. McGrath, G. E. Ballester, R. Yelle, *Science* **288**, 1208 (2000).
15. A. G. Davies et al., *Lunar Planet. Sci.* **XXX** (1999) [CD-ROM].
16. L. Keszthelyi and A. S. McEwen, *Geophys. Res. Lett.* **24**, 2463 (1997).
17. C. B. Phillips, dissertation, University of Arizona, Tucson, AZ (2000).
18. L. Keszthelyi, A. S. McEwen, Th. Thordarson, *J. Geophys. Res.*, in press.
19. J. R. Spencer et al., *Science* **288**, 1198 (2000).
20. S. Thorarinnsson, *Bull. Volcanol.* **2**, 1 (1953).
21. D. A. Williams, A. H. Wilson, and R. Greeley, *J. Geophys. Res.* **105**, 1671 (2000); D. A. Williams et al., *Eos* (spring meet. suppl.), in press.
22. K. Hon et al., *Geol. Soc. Am. Bull.* **106**, 251 (1994); B. C. Bruno, G. J. Taylor, S. K. Rowland, P. G. Lucey, S. Self, *Geophys. Res. Lett.* **19**, 305 (1992).
23. T. N. Mattox, C. Heliker, J. Kauahikaua, K. Hon, *Bull. Volcanol.* **55**, 407 (1993).
24. R. Lopes-Gautier et al., *Science* **288**, 1201 (2000).
25. S. W. Kieffer et al., *Science* **288**, 1204 (2000).
26. D. S. Acton, M. E. Brown, B. F. Lane, in preparation.
27. J. A. Stansberry, J. R. Spencer, R. R. Howell, C. Dumas, D. Vakil, *Geophys. Res. Lett.* **24**, 2455 (1997).
28. S. A. Fagents, D. A. Williams, R. Greeley, *Eos* (fall meet. suppl.) **80** (no. 46), F625 (1999).
29. L. Wilson and J. W. Head, *Nature* **302**, 663 (1983); J. W. Head and L. Wilson, *Lunar Planet. Sci.* **XXXI** (2000) [CD-ROM].
30. S. W. Kieffer, in *Satellites of Jupiter*, D. Morrison, Ed. (Univ. of Arizona Press, Tucson, AZ, 1982), pp. 647–723.
31. S. E. Heslop, L. Wilson, H. Pinkerton, J. W. Head, *Bull. Volcanol.* **51**, 415 (1989).
32. J. S. Kargel, P. Delmelle, D. B. Nash, *Icarus* **142**, 249 (1999).
33. P. M. Schenk and M. H. Bulmer, *Science* **279**, 1514 (1998).
34. The compressive stress induced by globally uniform subsidence exceeds 1 kbar at a depth of 2.5 km. For comparison, the stresses induced by tides are expected to be between 2 and 6 bar.
35. J. M. Moore, R. J. Sullivan, R. T. Pappalardo, E. P. Turtle, *Lunar Planet. Sci.* **XXXI** (2000) [CD-ROM].
36. J. F. McCauley, B. A. Smith, L. A. Soderblom, *Nature* **280**, 736 (1979).
37. S. Self, Th. Thordarson, L. Keszthelyi, in *Large Igneous Provinces: Continental, Oceanic, and Planetary Flood Volcanism*, J. J. Mahoney and M. F. Coffin, Eds. (American Geophysical Union, Washington, DC, 1997), pp. 381–410.
38. We thank J. Erickson and the Galileo team at JPL for their spacecraft recovery efforts during I24 and I25 and G. Levanus and G. Wells of JPL for the I24 image reconstruction.

8 February 2000; accepted 18 April 2000

Io's Thermal Emission from the Galileo Photopolarimeter-Radiometer

John R. Spencer,^{1*} Julie A. Rathbun,¹ Larry D. Travis,² Leslie K. Tamppari,³ Laura Barnard,³ Terry Z. Martin,³ Alfred S. McEwen⁴

Galileo's photopolarimeter-radiometer instrument mapped Io's thermal emission during the I24, I25, and I27 flybys with a spatial resolution of 2.2 to 300 kilometers. Mapping of Loki in I24 shows uniform temperatures for most of Loki Patera and high temperatures in the southwest corner, probably resulting from an eruption that began 1 month before the observation. Most of Loki Patera was resurfaced before I27. Pele's caldera floor has a low temperature of 160 kelvin, whereas flows at Pillan and Zamama have temperatures of up to 200 kelvin. Global maps of nighttime temperatures provide a means for estimating global heat flow.

The photopolarimeter-radiometer (PPR) is a simple aperture photometer on the Galileo scan platform, with a selection of broadband infrared

filters including a wide-open filter that is sensitive to light over the full visible to 100- μ m sensitivity range of the detector (*I*). During the close flybys (2), PPR obtained both dedicated raster scans of Io and "ride-along" sequences of data obtained simultaneously with the near-infrared mapping spectrometer (NIMS) or solid-state imaging (SSI) instruments. Calibration is with reference to dark sky and an onboard calibration source, and we estimate brightness temperatures (T_B 's) to be accurate to within 10 K at 250 K and 5 K at 125 K (3).

¹Lowell Observatory, 1400 West Mars Hill Road, Flagstaff, AZ 86001, USA. ²Institute for Space Studies, NASA-Goddard Space Flight Center, 2880 Broadway, New York, NY 10025, USA. ³Jet Propulsion Laboratory, 4800 Oak Grove Drive, Pasadena, CA 91109, USA. ⁴Lunar and Planetary Laboratory, University of Arizona, Tucson, AZ 85721, USA.

*To whom correspondence should be addressed. E-mail: spencer@lowell.edu